Electronic Supplementary Information (ESI)

A novel high-fluorescent S, N, O co-doped carbon dots for biosensing and bioimaging of copper ions in live cells

Yan-yu Dai,[‡a] Zhi-chao Liu,[‡c] Yun-feng Bai,[*b] Ze-zhong Chen,[b] Jun Qin[b] and Feng Feng[*ab]

[a] College of Chemistry and Chemical Engineering, Shanxi University, Taiyuan 030006, P.R. China.

[b] College of Chemistry and Environmental Engineering, Shanxi Datong University, Datong 037009, P. R. China.

[c] Institute for Advanced Study and Department of Chemistry, Nanchang University, Nanchang 330031, P. R. China.

*Corresponding author. Tel: +86-352-7158662; Fax: +86-352-6100028; E-mail: feng-feng64@263.net

‡ These authors contributed equally to this work.

Fig. S1. Plots of integrated fluorescence intensity against absorbance of Rhodamine 6G, S, N, O-CDs and undoped CDs at 460 nm.

Fig. S2. (A) XPS survey spectrum of S, N, O-CDs. (B) High resolution XPS survey spectrum of C 1s. (C) High resolution XPS survey spectrum of N 1s. (D) High resolution XPS survey spectrum of O 1s.

Fig. S3. FT-IR spectrum of S, N, O-CDs.

Fig. S4. The fluoresence quenching of S, N, O-CDs after additon of 100 μM Cu^{2+} for different times.

Fig. S5. UV-Vis spectra of m-PD, Cu^{2+}, S, N, O-CDs and the mixture of S, N, O-CDs and Cu^{2+} (S, N, O-CDs/Cu^{2+}).

Fig. S6. Fluorescence response of S, N, O-CDs towards common anion.

Fig. S7. Comparison of S, N, O-CDs after adding various amino acids.

Fig. S8. Cytotoxicity testing results of S, N, O-CDs on Hela cells viability. The values represent percentage cell viability (mean% ±SD, n=6).

Fig. S9. The fluoresence of mixture of S, N, O-CDs and 100 μM Cu^{2+} after additon of 200 μM PPi for different times.

Fig. S10. Fluorescence response of S, N, O-CDs towards different potential interferences in the presence of 100 μM Cu^{2+}. The concentrations of PPi and potential interferences were 200 μM and 0.1 M, respectively. F_0 and F represent the fluorescence of S, N, O-CDs in the absence of PPi and in the presence of PPi or potential interferences.

Fig. S11. The fluoresence of mixture of S, N, O-CDs, 100 μM Cu^{2+} and 200 μM PPi after additon of 160 U/L ALP for different times.

Fig. S12. Fluorescence response of S, N, O-CDs towards different potential interferences in the presence of 100 μM Cu^{2+} and 200 μM PPi. The concentrations of ALP or potential interferences was 160 U/L, respectively. F_0 and F represent the fluorescence of S, N, O-CDs in the absence of ALP and in the presence of ALP or potential interferences.

Table S1. Comparison of fluorescence quantum yield of different carbon dots.

Table S2. Comparison of limit detection of CDs-based Cu^{2+} probes.

Table S3. Detection of PPi and ALP in human urine samples or serum samples.

Fluorescence Quantum Yield (Φ_s) Measurement: Rhodamine 6G is chosen as a standard (Photochemistry and photobiology, 1969, 9: 439-444). The optical densities were measured on a Lambda 35 UV-vis spectrometer spectrophotometer. Absolute values are calculated using the standard reference sample that has a fixed and known fluorescence quantum yield value, according to the following equation:

$$\Phi_X = \Phi_{ST} (M_X/M_{ST})(\eta_X/\eta_{ST})^2$$

Where the subscripts ST and X denote standard and determinand samples respectively, Φ is the quantum yield, M is the gradient of integrated fluorescence vs. absorbance, and η is the refractive indices of the solvents.

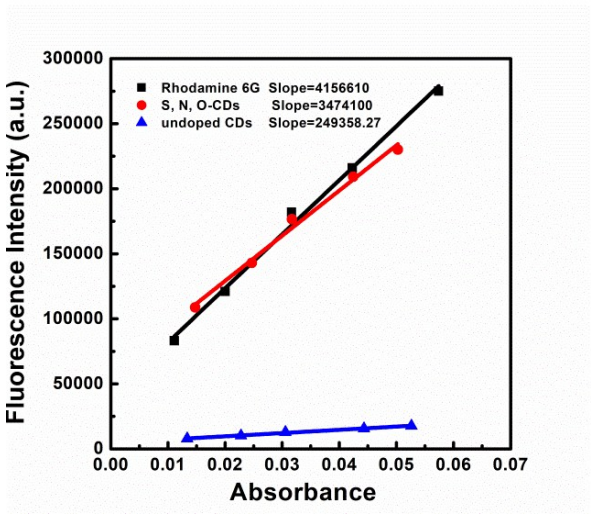

Fig. S1. Plots of integrated fluorescence intensity against absorbance of Rhodamine 6G, S, N, O-CDs and undoped CDs at 460 nm.

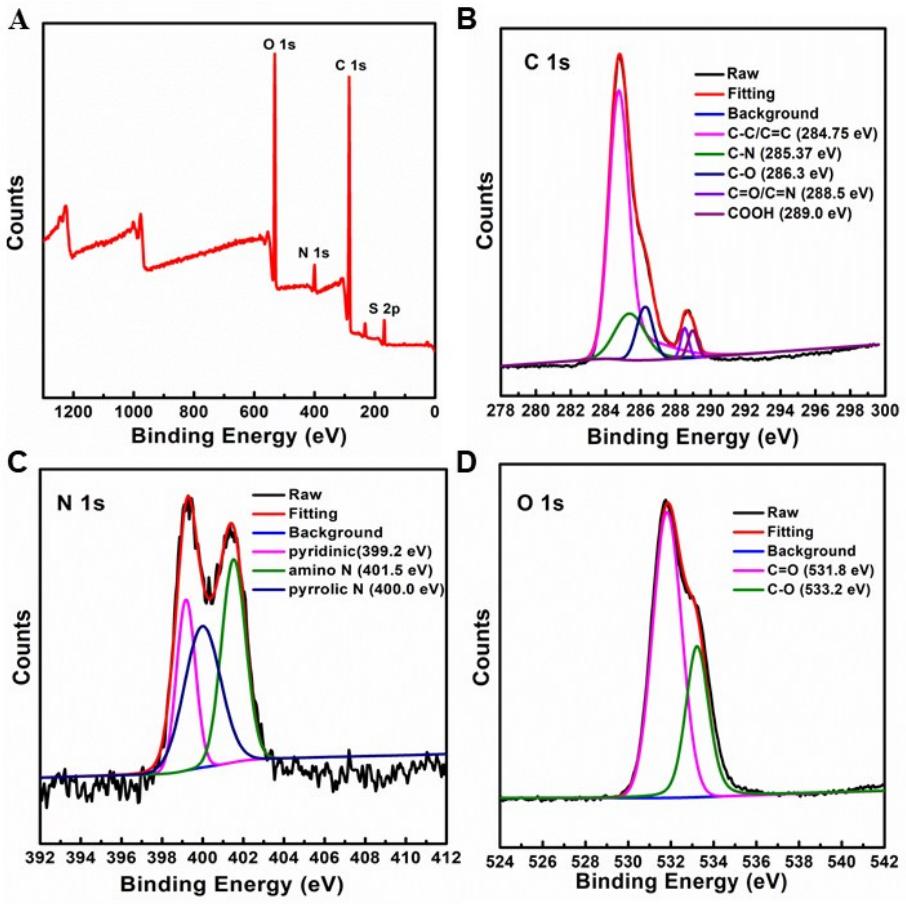

Fig. S2. (A) XPS survey spectrum of S, N, O-CDs. (B) High resolution XPS survey spectrum of C 1s. (C) High resolution XPS survey spectrum of N 1s. (D) High resolution XPS survey spectrum of O 1s.

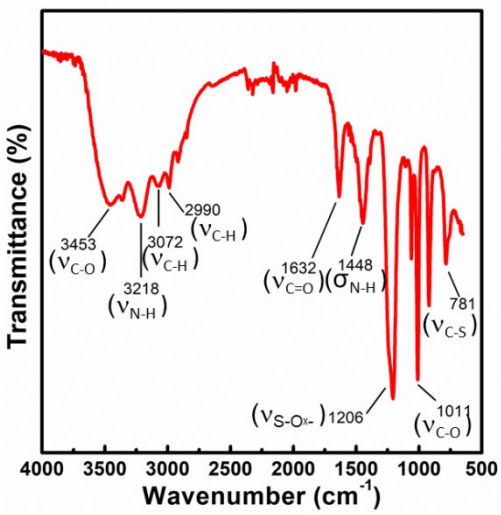

Fig. S3. FT-IR spectrum of S, N, O-CDs.

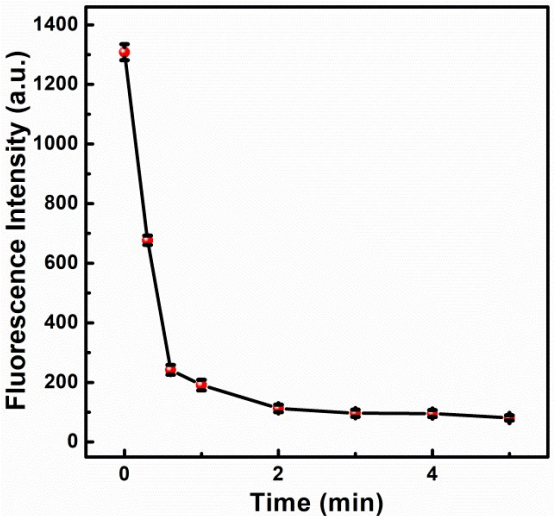

Fig. S4. The fluoresence quenching of S, N, O-CDs after additon of 100 μM Cu^{2+} for different times.

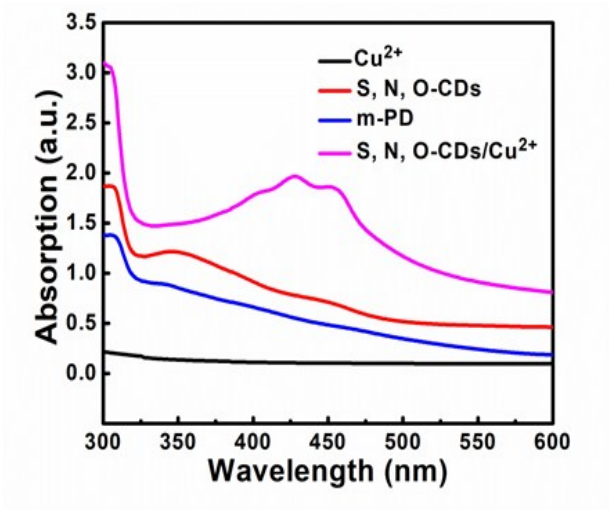

Fig. S5. UV-Vis spectra of m-PD, Cu^{2+}, S, N, O-CDs and the mixture of S, N, O-CDs and Cu^{2+} (S, N, O-CDs/Cu^{2+}).

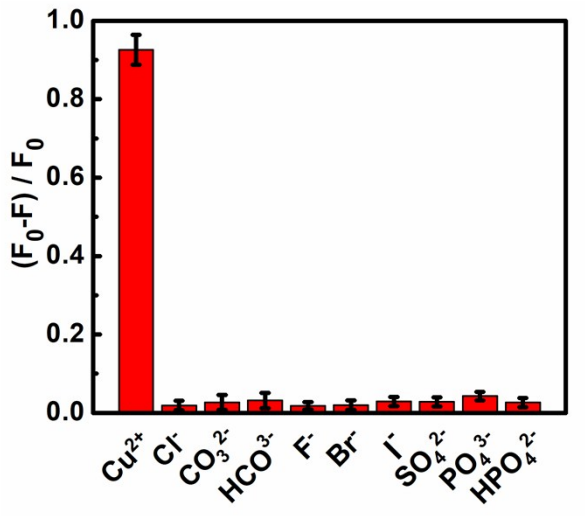

Fig. S6. Fluorescence response of S, N, O-CDs towards common anions.

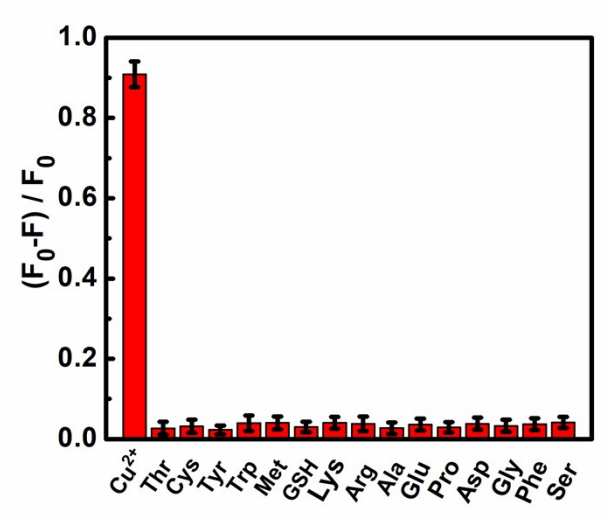

Fig. S7. Comparison of S, N, O-CDs after adding various amino acids.

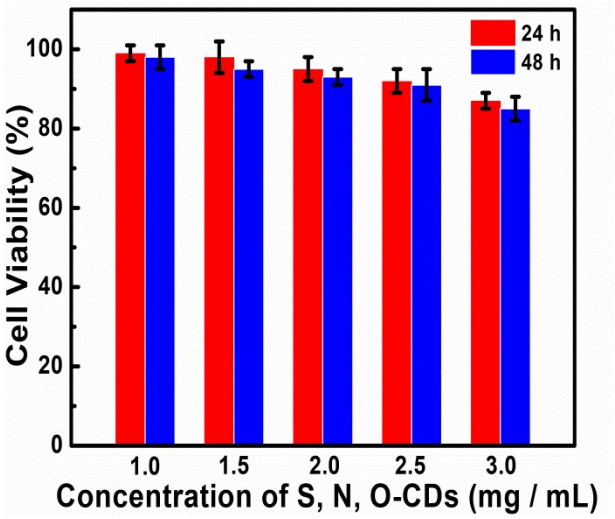

Fig. S8. Cytotoxicity testing results of S, N, O-CDs on Hela cells viability. The values represent percentage cell viability (mean% ±SD, n=6).

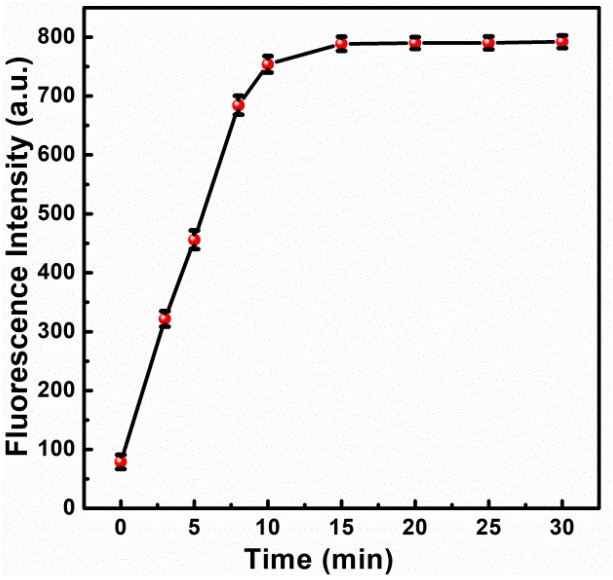

Fig. S9. The fluoresence of mixture of S, N, O-CDs and 100 μM Cu^{2+} after additon of 200 μM PPi for different times.

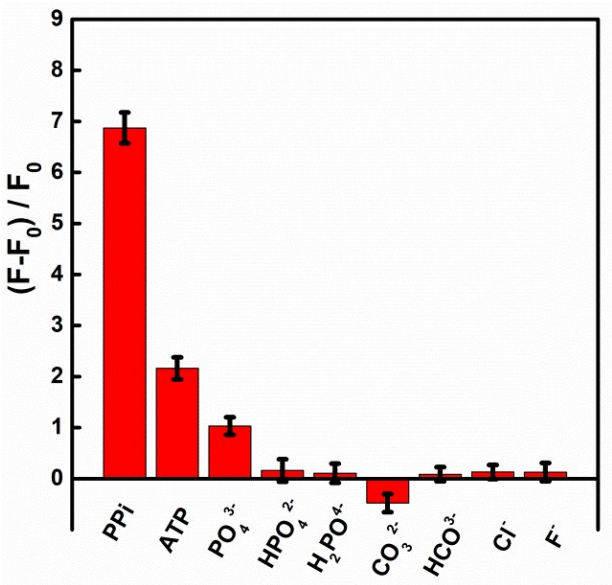

Fig. S10. Fluorescence response of S, N, O-CDs towards different potential interferences in the presence of 100 μM Cu^{2+}. The concentrations of PPi and potential interferences were 200 μM and 0.1 M, respectively. F_0 and F represent the fluorescence of S, N, O-CDs in the absence of PPi and in the presence of PPi or potential interferences.

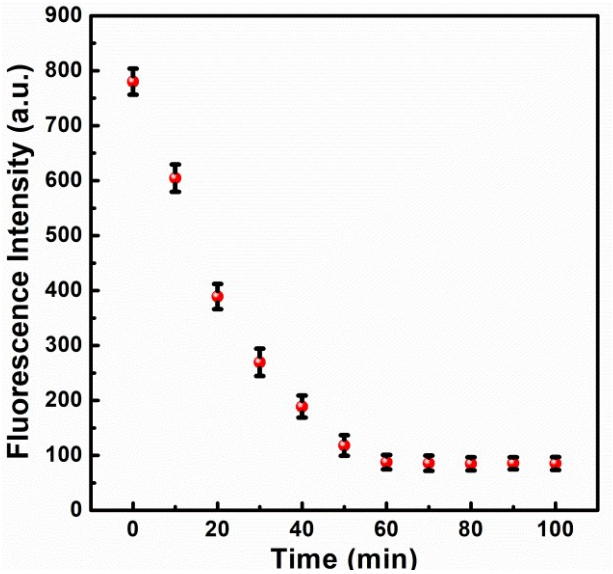

Fig. S11. The fluoresence of mixture of S, N, O-CDs, 100 μM Cu^{2+} and 200 μM PPi after additon of 160 U/L ALP for different times.

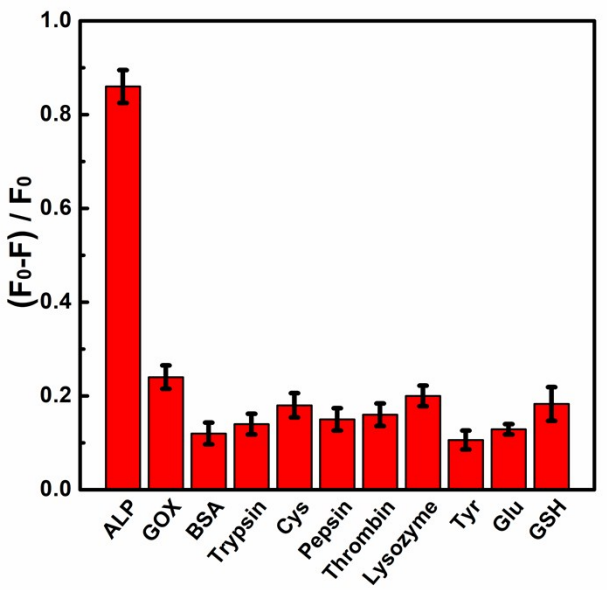

Fig. S12. Fluorescence response of S, N, O-CDs towards different potential interferences in the presence of 100 μM Cu^{2+} and 200 μM PPi. The concentrations of ALP or potential interferences was 160 U/L, respectively. F_0 and F represent the fluorescence of S, N, O-CDs in the absence of ALP and in the presence of ALP or potential interferences.

Table S1. Comparison of fluorescence quantum yield of different carbon dots [a].

Carbon dots	Standard Reference	Quantum Yield	Reference
S,N,O codoped	Quinine Sulfate	42.8%	S1
S,N,O codoped	Quinine Sulfate	21.6%	S2
N-doped	Rhodamine 6G	18.7%	S3
S,N,O codoped	Quinine Sulfate	73%	S4
N-doped	Rhodamine B	47%	S5
S-doped	Quinine Sulfate	5.77%	S6
S-doped	Quinine Sulfate	21.4%	S7
S,N,O codoped	Quinine Sulfate	63.8%	S8
S,N,O codoped	Rhodamine 6G	78.6%	this work

[a] The quantum yields (QY) of quinine sulfate (0.1 M H_2SO_4) at 350 nm and 366 nm excitation wavelength are 57.7% and 53%, respectively. Similarly, the QY of Rhodamine 6G in ethanol at 488 nm excitation wavelength is 94%. The QY of Rhodamine B using ethanol as a solvent are 69% and 89% under 365 nm and 495 nm excitation wavelength, respectively.

Table S2. Comparison of limit detection of CDs-based Cu^{2+} probes.

Fluorescent carbon dots (CDs)	**Limit of detection**	**Reference**
B, N-CDs	0.3 μM	S9
Calcium phosphate/CDs hybrid composites	9.82 μM	S10
CDs	4.8 μM	S11
CDs	0.76 μM	S12
CDs/polymeric matrix	0.71 μM	S13
Cyclam-functionalized CDs	0.1 μM	S14
Branched-polyethylenimize (BPEI)-capped CDs	0.115 μM	S15
S, N, O-CDs	0.29 μM	this work

Table S3. Detection of PPi and ALP in human urine samples or serum samples

Real samples	Added	Found	Recovery (%)	RSD (n=3, %)
Urine samples (PPi)	20 μM	38.78 μM	107.84	3.12
	40 μM	56.42 μM	97.28	4.44
	80 μM	100.89 μM	104.54	5.31
Serum samples (ALP)	20 U/L	18.95 U/L	94.73	5.13
	60 U/L	62.41 U/L	104.02	4.04
	100 U/L	104.72 U/L	104.72	4.51
	140 U/L	147.58 U/L	105.40	5.03

Reference

[S1] T. Chatzimitakos, A. Kasouni, L. Sygellou, I. Leonardos, A. Troganis and C. Stalikas, *Sens. Actuators*, B, 2018, **267**, 494-501.

[S2] W. Wang, Y.C. Lu, H. Huang, A.J. Wang, J.R. Chen and J.J. Feng, *Biosens. Bioelectron.*, 2015, **64**, 517-522.

[S3] X.Q. Li, Y.H. Zheng, Y.P. Tang, Q. Chen, J.W. Gao, Q. Luo and Q.M. Wang, *Spectrochim. Acta, Part A*, 2019, **206**, 240-245.

[S4] Y.Q. Dong, H.C. Pang, H.B. Yang, C.X. Guo, J.W. Shao, Y.W. Chi, C.M Li and T. Yu, *Angew. Chem. Int. Ed.*, 2013, **52**, 7800-7804.

[S5] M.Y. Li, C. Yu, C. Hu, W.B. Yang, C.T. Zhao, S. Wang, M.D. Zhang, J.Z. Zhao, X.N. Wang and J.S. Qiu, *Chem. Eng. J.*, 2017, **320**, 570-575.

[S6] V.M. Naik, D.B. Gunjal, A.H. Gore, S.P. Pawar, S.T. Mahanwar, P.V. Anbhule and G.B. Kolekar, *Diamond Relat. Mater.*, 2018, **88**, 262-268.

[S7] F. Nemati, M. Hosseini, R. Zare-Dorabei, F. Salehnia and M.R. Ganjali, *Sens. Actuators, B*, 2018, **273**, 25-34.

[S8] S. Liao, X.Y. Zhao, F.W. Zhu, M. Chen, Z.L. Wu, X.Z. Song, H. Yang and X.Q. Chen, *Talanta*, 2018, **180**, 300-308.

[S9] M. C. Rong, K. X. Zhang, Y. R. Wang and X. Chen, *Chin. Chem. Lett.*, 2017, **28**, 1119-1124.

[S10] S. Guo, S. Lu, P. X. Xu, Y. Ma, L. Zhao, Y. Zhao, W. Gu and M. Xue, *Dalton Trans.*, 2016, **45**, 7665-7671.

[S11] X. H. Ma, Y. H. Dong, H. Y. Sun and N. S. Chen, *Mater. Today Chem.*, 2017, **5**, 1-10.

[S12] V. A. Moreira, W. T. Suarez, M. D. O. K. Franco and F. F. Gambarra Neto, *Anal. Methods*, 2018, **10**, 4570-4578.

[S13] S. A. R. Shahamirifard, M. Ghaedi, M. Montazerozohori and A. Masoudiasl, *Photochem. Photobiol. Sci.*, 2018, **17**, 245-255.

[S14] J. Chen, Y. Li, K. Lv, W. B. Zhong, H. Wang, Z. Wu, P. G. Yi and J. H. Jiang, *Sens. Actuators, B*, 2016, **224**, 298-306.

[S15] Y. S. Liu, Y. N. Zhao and Y. Y. Zhang, *Sens. Actuators, B*, 2014, **196**, 647-652.